Active flutter suppression of a cantilever plate at supersonic speeds

A. BARAI, S. RAJA AND P. RAJAGOPAL

Structures Division, National Aerospace Laboratories, Bangalore 560 017, India

Modern high-speed aircrafts are flown using the fly-by-wire system. The dynamics of automatic flight control system interacts with aircraft's structural dynamics and aerodynamics to give rise to aeroservoelastic problems. Such problems can be avoided using an active control system. As a feasibility study, active flutter suppression of a cantilever plate wing was carried out. In this study it was demonstrated that the flutter Mach number of the cantilever wing can be increased by 12.5%.

Notations

a_i	Constants defined in Equation (20)
A, A_c	Co-efficient matrix in state-space form
A_R, A_I	Real and imaginary parts of unsteady aerodynamic force coefficient matrix
A_{Ra}, A_{Ia}	Real and imaginary parts of unsteady aerodynamic force coefficient matrix associated with control surface motion
b	Reference semi-chord
C_i	Constants defined in Equation (19)
D_i	Constants defined in Equation (22)
I	Unit matrix
k	Reduced frequency
K	Stiffness matrix
K_0	Control system gain
K_a	Coupling stiffness matrix for control surface degrees of freedom
M	Mach number
[M]	Mass matrix
M_a	Coupling mass matrix for control surface degrees of freedom
$p(s)$	Polynomial in s, defined in Equation (11)
Q_R, Q_I	Real and imaginary parts of unsteady aerodynamic force coefficients matrices

$q(t)$	Generalized coordinate
$q, \dot{q}$	Generalized velocity and acceleration
q_a	Generalized coordinate associated with control surface deflection
q_c	Control law command to the actuator
s	Laplace variable
t	Time
U	Free-stream velocity
X	Vector defined in Equation (23)
z	Plate response at node # 19

Greek symbols

ρ	Air density
ω	Frequency of oscillation (rad/s)
$\omega_b, \omega_t, \omega_c$	Bending, torsional and actuator response frequency (rad/s)
$\zeta_b, \zeta_t, \zeta_c$	Bending, torsional and actuator damping coefficients

Introduction and literature survey

During flight through atmosphere, the structural components of aerospace vehicles deform in a time-dependent fashion and produce motion-dependent unsteady aerodynamic forces which are responsible for dynamic aeroelastic instability – flutter, which leads to catastropic failure of vehicle components. This occurs due to interaction between elastic, inertia and unsteady aerodynamic forces. Several passive methods were being used in the past, but the recent technological advances in the field of control theory and availability of highly reliable control system electronic hardware offer a new way of treating the problem of flutter instability. This approach consists of a rapidly responding control system which is actuated by the motion of the main surface and which leads to appropriate deflection of the control surface. In this way, when the control surface aerodynamic forces are used to suppress flutter instability; this is known as *active flutter suppression* and the whole system is referred to as *active control system* (ACS). Studies have shown that sizeable weight savings are possible by using active flutter suppression as opposed to the normal passive flutter control method. In application, active controls employ various sensors, appropriately located on the vehicle to detect the deformation or motions, with suitable servo. feedback to accomplish the desired objectives. Figure 1*a*, shows a simplified general schematic; there can be multiple inputs and outputs, separate or combined systems, and onboard microcircuit computers.

Active control technology implies the intentional use of an aircraft of automatic control system. The system involves feedback control rather than passive aerodynamic design feature and is used to drive a number of specific control surfaces and possibly auxiliary force and moment generators. These controls improve the structural behaviour

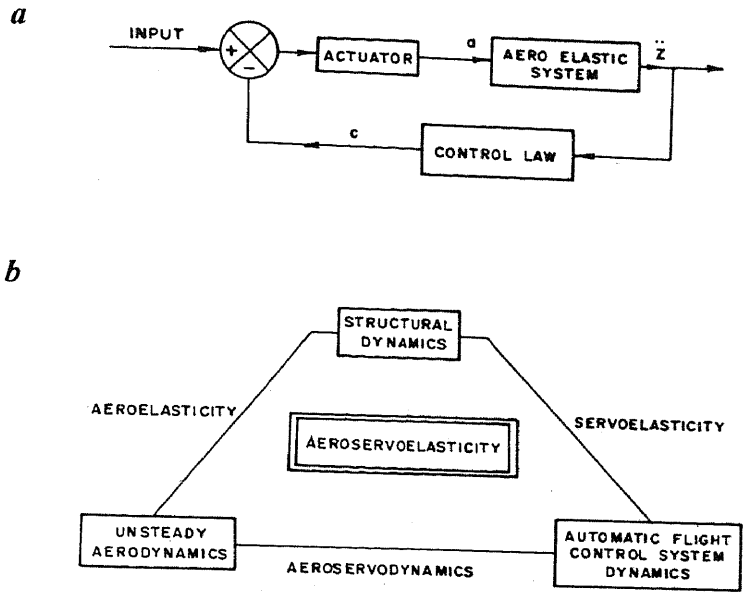

Figure 1. (a) Block diagram of the active control system; (b) aeroservoelastic interaction triangle.

of the aircraft and dynamic characteristics of its flight. The advanced control system refers to a devices that directly produces a change in the motion of the airplane. This includes automatic (no pilot's action required) as well as manual system. The systems or devices referred to may be flight critical, i.e., necessary for continued safe flight. Analytical ACT studies have indicated that the most significant performance improvements are achieved from six control functions:

1. Augmented stability (AS)
2. Gust load alleviation (GLA)
3. Manoeuvre load control (MLC)
4. Fatigue reduction (FR)
5. Ride control (RC)
6. Flutter mode control (FMC)

A good description of these is given by Shomber *et al.*[3]

The flexibility of aircraft not only leads to several aeroelastic problems, but also large amplitude motion due to structural deformation which is comparable with rigid body motion like pitch and plunge. Most of the recent configurations are statically unstable and

are controlled by automatic flight control systems. For these aircraft, the frequencies of the lower elastic modes and rigid-body modes are quite close. They interact in the presence of actuator mechanism of the flight control system (or active control system) and lead to instability known as aeroservoelastic (or ASE) instability. The ASE instability occurs due to interaction between an aircraft structural dynamics, aerodynamics and automatic flight control system (Figure 1*b*). The ASE entered into the aircraft design with the increased demand for minimum structural weight to meet strength requirements and by the use of high-authority, high-response, automatic flight control system to improve aircraft performance, stability, service life, ride quality, etc.

Radovich has classified the aeroservoelastic problems in the following way:

1. Steady aerodynamic, low-order servodynamics, structural elasticity in stability derivatives.
2. Steady manoeuvre involves steady aerodynamics, zero-order servodynamics and structural elasticity.
3. Unsteady aerodynamics, high-order servodynamics and accurate modelling of structural elasticity and aircraft inertia.

The aeroservoelasticity models are the analytical glue for all feedback control system and constitute the ACS's database for simulating the aircraft dynamics. The data cover structural deflection, aerodynamics, control surface details, sensor characteristics, servodynamics and active control computer definition, including control fluctuations and monitors. This paper deals with one of the ASE problem, namely, active flutter suppression.

For the design of an active control system, various approaches can be used. In the case of active flutter suppression system, the classical design technologies are based either on the application of the root locus method[6,7], frequency response method[8] and optimal control theory techniques[9,10]. There are other less conventional design techniques such as Nissim's aerodynamic energy concept[1] and the method of fictitious structural modifications[11] which can be applied as well.

For the design of an active flutter suppression system, it is necessary to formulate the equations of motion in Laplace domain. The structural-dynamic equations can be written in Laplace domain easily. Unsteady aerodynamic forces are normally calculated in frequency domain for a particular combination of Mach number (M) and reduced frequency (k). Therefore, the main problem in deriving equations of motion for active flutter suppression is to convert the tabular form of aerodynamic data into continuous function in the Laplace domain. Several methods are available in the literature for this purpose[12–16]. The cumbersome process of getting unsteady aerodynamic loads could be avoided in supersonic regime if piston theory is used. While using this theory, the complex generalized force coefficient matrix is evaluated for a given value of M and k. For fixed value of M, the real part remains constant but the imaginary part varies linearly with k. When the imaginary part is multiplied by $1/k$, it remains constant for all k. In this way, at constant altitude, the unsteady aerodynamic force coefficients are made to vary with Mach numbers. In this paper a cantilever plate with control surface is considered for

active flutter suppression study at supersonic speeds. The control system characteristics and actuator dynamics are represented similar to that of Reference 17. The equations of motion are derived in state-space form with and without active control system. Flutter characteristic of this configuration has been studied in References 18 and 19 without application of a control system. The flutter stability margin is determined using the root locus technique. The present study is an extension of the above studies for active flutter suppression.

Theoretical analysis

Equations of motion without the control system on

The equations of motion of lifting surfaces in flight in modal coordinate are given by

$$[M]\{\ddot{q}\} + [K]\{q\} = [Q]\{q\} \tag{1}$$

where $[M]$ is the generalized mass matrix (diagonal), $[K]$ is the generalized stiffness matrix (diagonal) and $[Q]$ is matrix of generalized aerodynamic force coefficients. Now, Equation (1) can also be written in the following form:

$$[M]\{\ddot{q}\} + [K]\{q\} = -(1/2)\,\rho\, U^2\,[Q_R + Q_I]\{q\}$$

$$= -(1/2)\,\rho\, U^2 [Q_R]\{q\} - (1/2)\,\rho\, Ub\left(\frac{U}{\omega b}\right)[Q_I]\{i\omega q\}$$

$$= -[A_R]\{q\} - (1/k)\,[A_I]\{\dot{q}\}$$

or

$$[M]\{\ddot{q}\} + [K]\{q\} + [A_R]\{q\} + (1/k)\,[A_I]\{\dot{q}\} = 0$$

or

$$\{\ddot{q}\} + (1/k)\,[M^{-1}A_I]\{\dot{q}\} + [M^{-1}K + M^{-1}A_R]\{q\} = 0 \tag{2}$$

Let

$$\dot{q} = x \tag{3a}$$

and

$$\ddot{q} = \dot{x} \tag{3b}$$

Now Equation (2) can be written in state-variable form as

$$\{\dot{x}\} = -(1/k)[M^{-1}A_I]\{x\} - [M^{-1}K + M^{-1}A_R]\{q\} \tag{4}$$

Combining Equations (3a) and (4) one can write

$$\begin{Bmatrix} \dot{q} \\ \dot{x} \end{Bmatrix} = \begin{bmatrix} 0 & I \\ -M^{-1}K - M^{-1}A_R & -(1/k)M^{-1}A_I \end{bmatrix} \begin{Bmatrix} q \\ x \end{Bmatrix} \tag{5}$$

The above equation can be written as

$$\dot{X} = A\,X \tag{6}$$

where

$$A = \begin{bmatrix} 0 & I \\ -M^{-1}K - M^{-1}A_R & -(1/k)M^{-1}A_I \end{bmatrix} \tag{7}$$

Equation (6) is solved as an eigenvalue problem for a range of Mach numbers. Since A is unsymmetric, the eigenvalue of A is in general complex. They are calculated using some standard subroutine on unsymmetric matrix eigenvalue extraction.

Equations of motion with control system on

In this section, the equations of motion is derived for the lifting surface with an active control system. To achieve this, it is necessary to incorporate the actuator transfer function and an appropriate control law into the equation of motion. The block diagram of the active control system is shown in Figure 1*a*. The frequency response function of the actuator in Laplace domain is given by

$$\frac{q_a}{q_c} = \frac{K_0}{(s^2 + 2\omega_b\zeta_b s + \omega_b^2)(s^2 + 2\omega_t\zeta_t s + \omega_t^2)} \tag{8}$$

where q_a is the control surface deflection, q_c is the control command to the actuator and K_0 is the control law gain parameter. The next step is to use a control law to demonstrate at least 10% increase in critical flutter Mach number over that of the passive wing. For this purpose, the transfer function of the control system (also known as control law) is chosen as[17].

$$\frac{q_c}{\ddot{z}} = \frac{1}{(s^2 + 2\omega_c\zeta_c s + \omega_c^2)} \tag{9}$$

Therefore, the transfer function of the active control system as a total is given by combining Equations (8) and (9) as

$$\frac{q_a}{\ddot{z}} = \frac{q_c}{\ddot{z}}\,\frac{q_a}{q_c} \tag{10}$$

$$= \frac{K_0}{(s^2 + 2\omega_b\zeta_b s + \omega_b^2)(s^2 + 2\omega_t\zeta_t s + \omega_t^2)(s^2 + 2\omega_c\zeta_c s + \omega_c^2)}$$

$$= \frac{K_0}{p(s)} \tag{11}$$

Now from Equation (1) one can write

$$[M:M_a]\begin{Bmatrix}\ddot{q}\\ \ddot{q}_a\end{Bmatrix} + [K:K_a]\begin{Bmatrix}q\\ q_a\end{Bmatrix} = -(1/2)\rho U^2 [Q:Q_a]\begin{Bmatrix}q\\ q_a\end{Bmatrix} \tag{12}$$

where M_a, K_a and Q_a are control surface inertia, stiffness and aerodynamic coupling matrices, respectively. In the present study M_a and K_a matrices are omitted. Equation (12) can be written like Equation (2) as

$$[M]\{q\} + [K]\{q\} = -[\bar{A}_R]\{q\} - (1/k)[\bar{A}_I]\{q\} - [\bar{A}_{Ra}]\{q_a\} - (1/k)[\bar{A}_{Ia}]\{q_a\} \tag{13}$$

or

$$[M]\{\ddot{q}\} - [A_I]\{\dot{q}\} + [K - A_R]\{q\} - [A_{Ra}]\{q_a\} - [A_{Ia}]\{\dot{q}_a\}. \tag{14}$$

For a single control surface and a single sensor (accelerometer) the control law transfer function can be assumed to be of the form

$$\frac{Z(q_a)}{Z(\ddot{z})} = \frac{K_0}{p(s)} \tag{15}$$

or

$$(q_a) = \frac{s^2 K_0}{p(s)} z, \quad z = [T]\{q\} \tag{16}$$

where z can be related to q through a transfer matrix. Substituting Equation (16) into Equation (14) and the result in Equation (15), one can write

$$[[M]s^2 - [A_I]s + [K - A_R]]\{q(s)\} - [A_{Ra}]\frac{K_0 s^2}{p(s)}\{q_a\} - [A_{Ia}]\frac{K_0 s^3}{p(s)}\{q_a\} = 0$$

or

$$([[M]s^2 - [A_I]s + [K - A_R]]\, p(s) - [A_{Ra}]\, K_0 s^2 - [A_{Ia}]\, K_0 s^3)\{q\} = 0 \tag{17}$$

Substituting for $p(s)$ from Equation (11) in Equation (17), one can write

$$(Ms^8 + (C_1M - A_I)s^7 + [C_2M + (K - A_R) - C_1A_I]s^6 + [C_3M - C_2A_I + C_1(K - A_R)]s^5 + [C_4 - C_3A_I + C_2(K - A_R)]s^4 + [C_5M - C_4A_I + C_3(K - A_R) - A_{Ia}K_0]s^3 + [C_6M - C_5A_I + C_4(K - A_R) - A_{Ra}K_0]s^2 + [M - C_6A_I + C_5(K - A_I)]s + [C_6(K - A_R)]\}\{q\} = 0 \quad (18)$$

where

$$C_1 = a_5 + a_9; \quad C_2 = a_6 + a_5a_9 + a_{10}; \quad C_3 = a_7 + a_6a_9 + a_{10}$$
$$C_4 = a_8 + a_7a_9 + a_6a_{10}; \quad C_5 = a_8a_9 + a_7a_{10}; \quad C_6 = a_8a_{10} \quad (19)$$

and

$$a_1 = 2\omega_b\zeta_b; \quad a_2 = \omega_b^2; \quad a_3 = 2\omega_t\zeta_t; \quad a_4 = \omega_t^2$$
$$a_5 = a_1 + a_3; \quad a_6 = a_1 + a_4 + a_1a_3; \quad a_7 = a_1a_4 + a_2a_3$$
$$a_8 = a_2a_4; \quad a_9 = 2\omega_c\zeta_c; \quad a_{10} = \omega_c^2 \quad (20)$$

Equation (18) can also be written as

$$(D_1s^8 + D_2s^7 + D_3s^6 + D_4s^5 + D_5s^4 + D_6s^3 + D_7s^2 + D_8s + D_9)\{q\} = 0 \quad (21)$$

where

$$D_1 = M$$
$$D_2 = C_1M - A_I$$
$$D_3 = C_2M + (K - A_R) - C_1A_1$$
$$D_4 = C_3M + C_1(K - A_R) - C_2A_I$$
$$D_5 = C_4M + C_2(K - A_R) - C_3A_I \quad (22)$$
$$D_6 = C_5M + C_3(K - A_R) - C_4A_I - A_{Ia}K_0$$
$$D_7 = C_6M + C_4(K - A_R) - C_5A_I - A_{Ra}K_0$$
$$D_8 = C_5(K - A_R) - C_6A_I; \quad D_9 = C_6(K - A_R)$$

Equation (21) can be reduced to a series of first-order equations of the following form:

$$s\{X\}\{X\} = [A_c]\{X\} \quad (23)$$

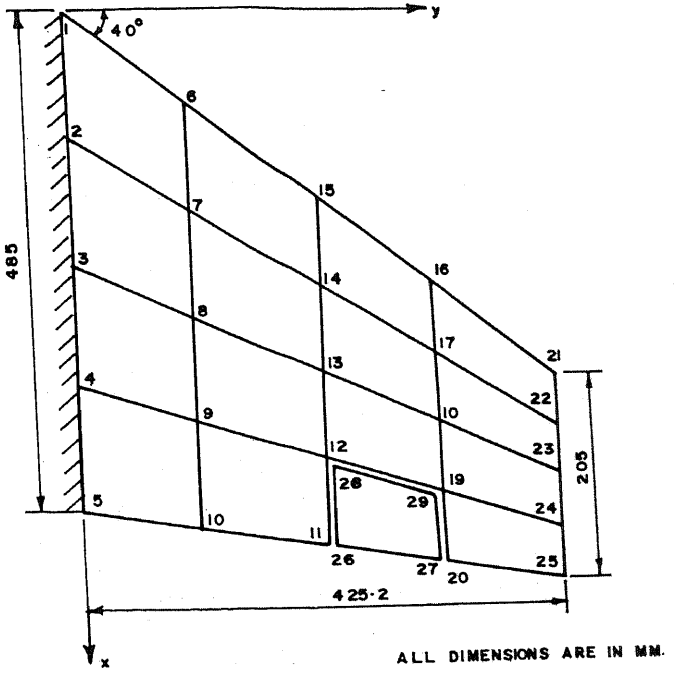

Figure 2. Finite-element model of the cantilever plate surface.

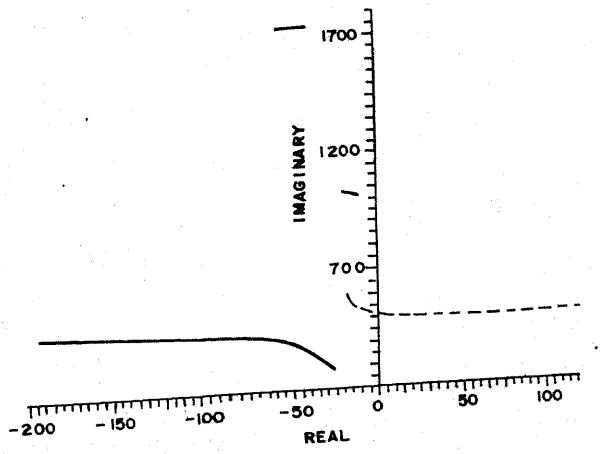

Figure 3. Root locus plot of flutter eigenvalue without control.

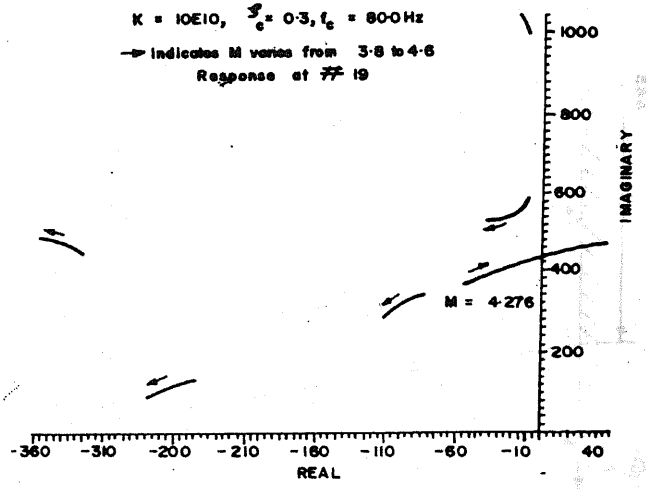
K = 10E10, ζ_c = 0·3, f_c = 80·0 Hz
Indicates M varies from 3·8 to 4·6
Response at # 19
M = 4·276
IMAGINARY
REAL
1000
800
600
400
200
-360
-310
-200
-210
-160
-110
-60
-10
40

a

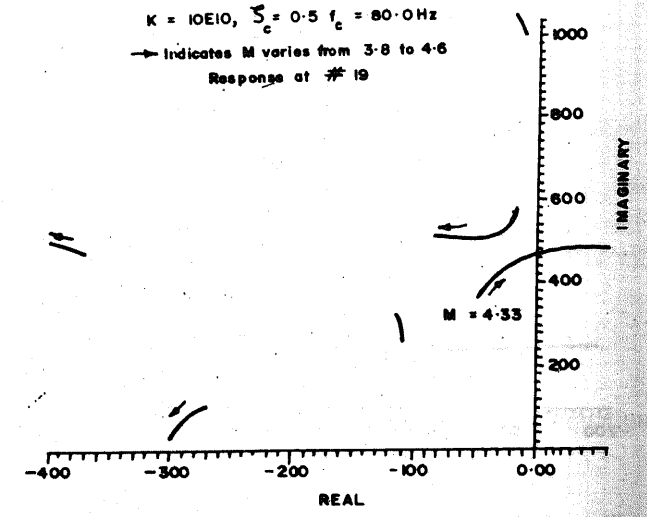
K = 10E10, ζ_c = 0·5 f_c = 80·0 Hz
Indicates M varies from 3·8 to 4·6
Response at # 19
M = 4·33
IMAGINARY
REAL
1000
800
600
400
200
-400
-300
-200
-100
0·00

b

cont

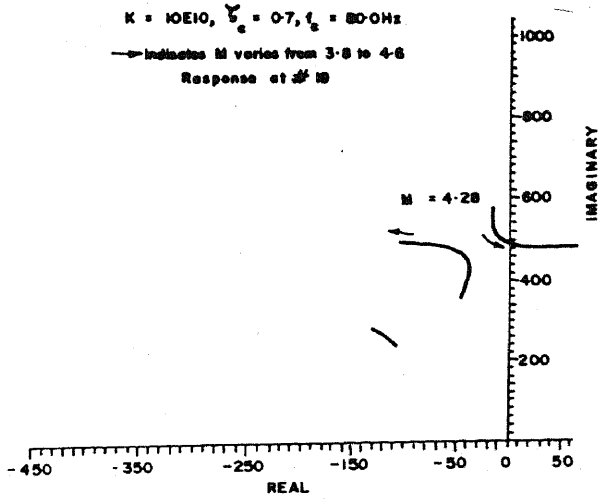

c

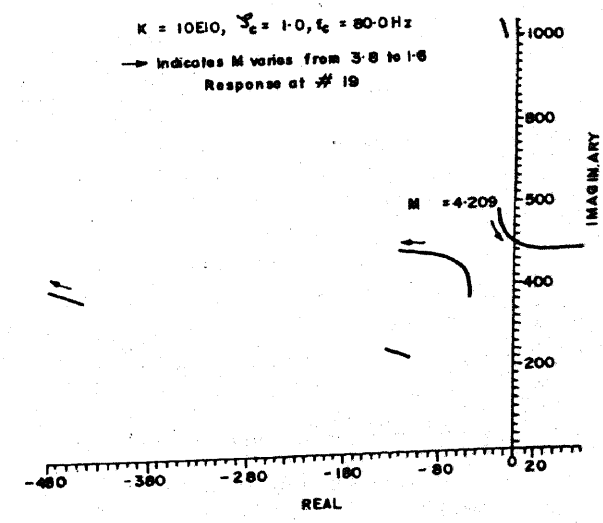

d

continued

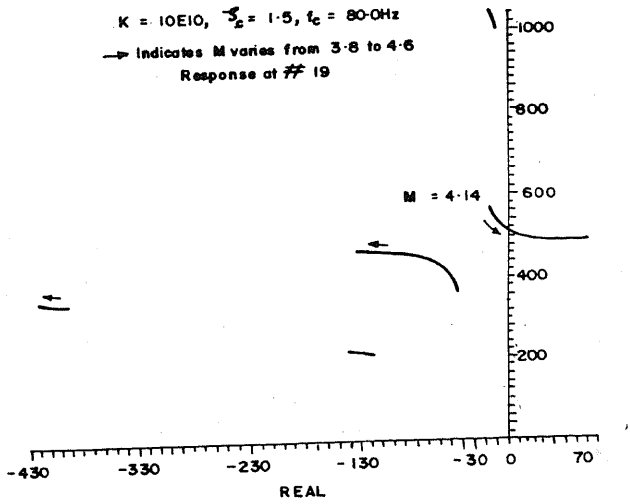

e

Figure 4. Root locus plot of flutter eigenvalue with control.

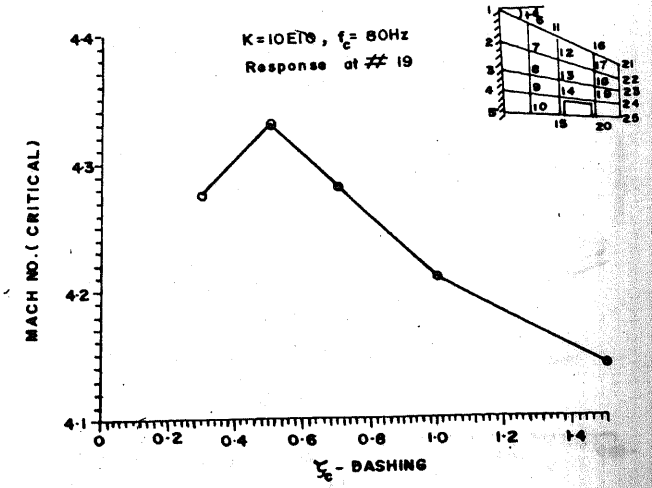

Figure 5. M_{cr} vs ζ_c curve.

where

$$X = \begin{Bmatrix} s^7\{q\} \\ s^6\{q\} \\ s^5\{q\} \\ s^4\{q\} \\ s^3\{q\} \\ s^2\{q\} \\ s^1\{q\} \\ s^0\{q\} \end{Bmatrix}$$

and

$$A_c = \begin{bmatrix} D_1^{-1}D_2 & D_1^{-1}D_3 & D_1^{-1}D_4 & D_1^{-1}D_5 & D_1^{-1}D_6 & D_1^{-1}D_7 & D_1^{-1}D_8 & D_1^{-1}D_9 \\ \mathrm{I} & 0 & 0 & 0 & 0 & 0 & 0 & 0 \\ 0 & \mathrm{I} & 0 & 0 & 0 & 0 & 0 & 0 \\ 0 & 0 & \mathrm{I} & 0 & 0 & 0 & 0 & 0 \\ 0 & 0 & 0 & \mathrm{I} & 0 & 0 & 0 & 0 \\ 0 & 0 & 0 & 0 & \mathrm{I} & 0 & 0 & 0 \\ 0 & 0 & 0 & 0 & 0 & \mathrm{I} & 0 & 0 \\ 0 & 0 & 0 & 0 & 0 & 0 & \mathrm{I} & 0 \end{bmatrix}$$

For a fixed value of air density (altitude) and velocity, the eigenvalues of Equation (23) are the roots of the characteristics equation. Root loci can be constructed which correspond to the variation of eigenvalues of the system as Mach number is varied.

Numerical calculations

For numerical calculations, a cantilever plate is considered. The geometry of the plate is shown in Figure 2. First, the flutter analysis for this configuration is made using NASTRAN package considering the control as an irreversible system (control surface is locked with main surface). In this process, the generalized mass, stiffness and aerodynamic matrices are also obtained. Three modes and the corresponding modal quantities (mass, stiffness and aerodynamic forces) are considered to formulate equations of motion and subsequent representation in state-variable form. The mass and stiffness matrices are real but the aerodynamic matrix is complex. Since piston theory is used, the real part is constant (independent of k) and imaginary part varies linearly with k. In the flutter equation (Equation (2) or (14)) the imaginary part of the unsteady aerodynamic force co-efficients remains constant when divided by the reduced frequency. Thus, the final flutter equation is solved by varying the Mach number while the density of air is kept constant for a particular altitude. Then the flutter equation is expressed in state-space form and the flutter stability analysis is carried out using the root locus technique. In this,

the real part of the complex eigenvalue at each Mach number is plotted against the imaginary part. The system is stable if a point lies on the left half of the imaginary axis. A point on the imaginary axis implies that the system is marginally stable. Therefore, a point just on right side of the imaginary axis is taken as initiation of flutter.

Results and discussion

The eigenvalues of Equation (6) are the roots of the characteristic flutter equation for the cantilever plate at sea level, without flutter suppression system. The root locus for increasing values of the Mach number (air speed), from 3.1 to 4.3, is presented in Figure 3. Arrows indicate the direction of increasing Mach number. The flutter instability occurs at $M_{cr} = 3.945$, where the, torsional mode becomes unstable.

The eigenvalues of Equation (23) are the roots of the characteristic flutter equation for the cantilever plate with a trailing edge control surface and active flutter suppression system. The inclusion of control system and actuator dynamics into the aeroelastic system changes the order of the system from second to eighth (Equation (21)).

The flutter speed with active control system on depends on three system parameters – gain of the control system (K_0), the frequency of actuator output (ω_c) and its damping (ζ_c). It was found that for some combination of K_0, ω_c and ζ_c, the critical flutter Mach number is lower than the system without active control system. Therefore, for a parametric study, any two of the above parameters are kept constant and the third one is varied. To

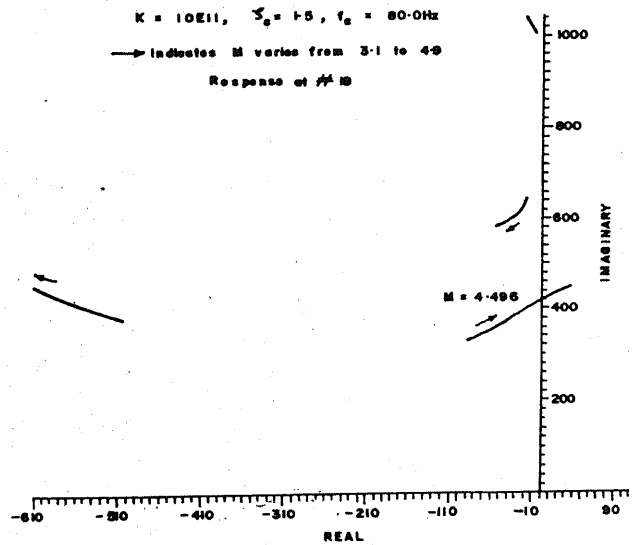

Figure 6. Root locus plot of flutter eigenvalue with control.

Table 1. Variation of flutter Mach number (M_{cr}) with control system gain K_0

K_0	M_{cr}
10E + 10	4.14
10E + 11	4.496
Without control	3.945

study the effect of actuator output frequency, K_0 and ω_c are kept constant. It is found that critical flutter Mach number is maximum when actuator output frequency is equal to the torsional frequency of the plate. Next, the effect of actuator damping is studied. The root locus plots for different values of damping are shown in Figures 4*a–e*. For low values of damping the first mode becomes unstable (Figures 4*a* and *b*) but for higher values of damping the second mode becomes unstable (Figures 4*c–e*). The critical Mach number for different values of damping is presented in Figure 5. It is clear from Figure 5 that the critical flutter Mach number is maximum when damping value is 0.5.

Finally, the effect of control system gain is studied and presented in Figure 6 for $\zeta_c = 1.5$ and $K_0 = 10E + 11$. The critical flutter Mach number of various gain is presented in Table 1.

Conclusions

The flutter characteristics of a cantilever plate, with and without an active flutter suppression system on, are studied in this paper. Since the flutter frequency and speed (at supersonic flow) are quite high, the actuator output frequency will have to be quite high. At present such actuators are not available. Therefore, the present study is a numerical experimentation and demonstration of active flutter suppression concept. It may not have any practical utility.

References

1. Nissim, E., Flutter suppression using active controls based on a concept of aerodynamic energy, NASA TN D-6199, Mar. 1971.
2. Thompson, G. O. and Kass, G. J., Active flutter suppression – an emerging technology, *J. Aircraft*, 1972, **9**, 230–235.
3. Schoenman, R. L. and Shomber, H. A., Impact of active controls on future transport design, performance and operation, SAE Paper 751051, *Trans. SAE*, 1975, **84**, Section 4, 2917–2932.
4. Ostgaard, M. A. and Swortzel, F. R., CCVs active control technology creating new military aircraft design potential, *Astron. Aeron.*, 1977, **15**, 42–51.
5. Hwang, C. and Kesler, D. F., Aircraft active controls – new era in design, *Astron. Aeron.*, 1983, **21**, 70–79, 85.
6. Horikawa, H. and Dowell, E. H., Elementary explanation of the flutter mechanism with active feedback controls, *J. Aircraft*, 1979, **16**, 225–232.
7. Hwang, C., Johnson, E. H. and Pi, W. S., Recent development of the YF-17 active flutter suppression system, *J. Aircraft*, 1981, **18**, 537–545.

8. Peloubet, P. R., Jr., Haller, R. L. and Bolding, R. M., F-16 Flutter suppression system investigation, *AIAA* Paper 80-0768, Paper presented at the 21st Structures, Structural Dynamics and Materials Conf., Seattle, Washington, May 1980, Part 2, pp. 620–634.
9. Newsom, J. R., A method for obtaining practical flutter suppression control laws using results of optimum control theory, NASA TP-1471, Aug. 1979.
10. Newsom, J. R., Control law synthesis for active flutter suppression using optimal control theory, *J. Guidance, Control and Dynamics*, 1979, **2**, 388–394.
11. Freymann, R., New simplified ways to understand the interaction between aircraft structures and active control system, *AIAA* Paper 84-1868, *AIAA* CP-848, 1984, 233–245.
12. Vepa, R., On the use of pade approximants to represent unsteady aerodynamic loads for arbitrarily small motions of wings, *AIAA* Paper 76-17, Jan. 1976.
13. Edwards, J. W., Unsteady aerodynamic modelling and active aeroelastic control, Ph.D. Dissertation, Dept. of Aeronautics and Astronautics, Stanford University, Calif. 1977, SUDAAR 504 (also NASA CR-148019).
14. Abel, I., An analytical technique for predicting the characteristics of a flexible wing equipped with an active flutter-suppression system and comparison with wind-tunnel data, NASA TP-1367, Feb. 1979.
15. Karpel, M., Design for active flutter suppression and gust alleviation using state-space aeroelastic modeling, *J. Aircraft*, 1982, **19**, 221–227.
16. Tiffany, S. H. and Adams, W. M., Jr., Nonlinear programming extensions to rational function approximation methods for unsteady aerodynamic forces, NASA TP-2776, July 1988.
17. Abel, I. and Newsom, J. R., Wind tunnel evaluation of NASA-developed control laws for flutter suppression on a DC-10 derivative wing, *NASA* TM 83143, Jan. 1981.
18. Kamesh, J. V., Madhusudhan, B. S. and Rajagopal, P., Analytical determination of the flutter characteristics of a lifting surface (without a control surface) using the root-locus plots, *NAL* TM ST 9102, Jan. 1991.
19. Kamesh, J. V., Madhusudhan, B. S., Rajagopal, P. and Vijaya Vittala, N. G., Determination of the flutter characteristics of a wing model using – a) airloads approximated by a rational polynomial in the transform variables, b) generalized airloads, *NAL* TM ST 9103, July 1991.